Chin. J. Astron. Astrophys. Vol. 6 (2006), No. 3, 363–371
(*http://www.chjaa.org*)

Chinese Journal of
Astronomy and
Astrophysics

Velocity Space of Galactic O-B Stars *

Zi Zhu

Department of Astronomy, Nanjing University, Nanjing 210093; *zhuzi@nju.edu.cn*

Received 2005 August 29; accepted 2005 September 16

Abstract Based on the Hipparcos proper motions and available radial velocity data of O-B stars, we have re-examined the local kinematical structure of the young disk population of $\sim$ 1500 O-B stars not including the Gould-belt stars. A systematic warping motion of the stars about the direction to the Galactic center has been reconfirmed. A negative *K*-term implying a systematic contraction of stars in the solar vicinity has been detected. Two different distance scales are used in order to find out their impact on the kinematical parameters, and we conclude that the adopted distance scale plays an important role in characterizing the kinematical parameters at the present level of the measurement uncertainty.

Key words: astrometry — Galaxy: kinematics and dynamics — stars: early-type — Galaxy: solar neighborhood

1 INTRODUCTION

Kinematical information of the local disks provides a crucial constraint for Galactic dynamical and mass models. During the last decade, a great deal of effort has been expended in studying the local kinematics of our Galaxy in response to the enormous progress made in the acquisition of high-quality observational data. The absolute stellar proper motions, radial velocities and trigonometric parallaxes are fundamental quantities to characterize the Galactic velocity fields in the solar vicinity. Because of the small velocity dispersion and small rotational lag relative to the LSR of the young disk population, which includes neutral hydrogen, O-B stars and supergiants, classical Cepheids, and young open clusters, the analysis of large scale velocity fields of objects that belong to the young Galactic disk is the principal tools used by many investigators.

It is found in the early investigation of the large scale distribution of H I gas in the Galaxy, that the H I gas layer has systematic deviations above the Galactic plane on one side and below it on the other side similar to many flat galaxies (Kerr 1957). This structure is called the Galactic warp. Young optical objects such as O-B stars have a very close relation to the H I gas, and are considered as an optical counterpart of the H I warp. Thus, they are expected to exhibit similar spatial distribution and kinematical behaviors as the H I gas. Analyzing the proper motions of O-B5 stars, supergiants and bright giants provided by ground-based astrometric catalogue ACRS (Astrographic Catalogue Reference Stars), a warping motion inherent in the Galactic warp was detected by Miyamoto et al. (1993). Based on stellar proper motions in the Hipparcos catalogue, Smart et al. (1998) and Drimmel et al. (2000) reported that the kinematics of the O-B stars toward the Galactic anti-center shows negative systematic motions as opposed to the expected positive motions. Carrying out a proper-motion analysis for Hipparcos O-B5 stars, Miyamoto & Zhu (1998) found a clear warping motion with a systematic rotation of $+3.8\pm1.1$ km s^{-1} kpc^{-1} for stars about the axis pointing to the Galactic center.

* Supported by the National Natural Science Foundation of China.

The space velocities of the stars in the solar neighborhood can be interpreted as an average rotation about the Galactic gravity center plus random motions (velocity dispersion). The epicyclic approximation of the stellar orbits in the Galactic plane states that the circular velocity is realized by the rotation of the LSR defined by an ideal sample of stars with a limiting velocity dispersion of zero. Such stellar systems are said to be dynamically cold. In the cold limit, the streaming is along the closed orbits supported by the gravitational potential. Thus, knowledge about the Galactic potential and the mass distribution of the Galaxy can be gained from the kinematical study. Since the young disk population of O-B stars and classical Cepheids yield the lowest velocity dispersion, the rotational velocity of the LSR defined by it gives the best approximation to the circular velocity at the Sun.

In the recent years, a great mass of work has been carried out in the kinematical analysis of the Galaxy, including using data of the very early type of stars as well as the late type giants. Among them, proper motion analysis was the usual way to characterize the kinematical structure of the Galaxy; few studies were based on radial velocity data due to the lack of available radial velocity measurements of useable size. The period-luminosity relation, subsequently extended into a period-luminosity-color relation, has made it possible to obtain reliable distances for the classical Cepheids. Radial velocity measurements, complemented with the photometric distance scales invited people to solve the local kinematical structure defined by the disk Cepheids, and yielded the Oort constant A and the galactocentric distance of the Sun R_0 (Caldwell & Coulson 1987; Pont et al. 1994; Pont et al. 1997; Metzger et al. 1998). Feast & Whitelock (1997) proposed the Cepheid period-luminosity relation derived from Hipparcos trigonometric parallaxes. The Oort constants were obtained from the proper motions of Cepheids observed by the Hipparcos satellite (Feast & Catchpole 1997). The Oort constants $A = 14.8\pm0.8$ km s^{-1} kpc^{-1} and $B = -12.4\pm0.6$ km s^{-1} kpc^{-1} given by Feast & Catchpole(1997) are consistent with those recommended by IAU 1985 (Kerr & Linden-Bell 1986), while significantly larger values for $A - B$ have been found from the proper motions analysis by several authors. The VLA observation of the proper motion of the compact radio source Sgr A*, which is generally thought to mark the Galactic center, gives $A - B = 28.5\pm0.9$ km s^{-1} kpc^{-1} (Backer & Sramek 1999). Even larger values for $A - B$ have been found by Olling & Dehnen (2003), derived from proper motions of the old red giants from ACT/Tycho-2 catalogues; by Méndez et al. (1999) and by Miyamoto & Zhu (1998), based on stellar proper motions from the Southern Proper Motion Program and the Hipparcos O-B5 stars.

In our previous work, using the Hipparcos proper motion supplemented with radial velocity data, we have performed a kinematical study of the Cepheids, and found a negative K-term which implies a Galactic contraction in the solar neighborhood (Zhu 2000). The reality of this contraction is still doubtful. In the present work, we concentrate our effort on an analysis of the young disk population of O-B stars on the basis of the transverse velocity data combined with the radial velocity data, in order to re-examine the Galactic warping motion found before (cf. Miyamoto & Zhu 1998) and the local contraction of the young disk population.

2 KINEMATICAL MODEL

In the early part of the last century, Lindblad and Oort developed a simple axisymmetric model to characterize the local kinematics of stars of the solar vicinity. They actually considered that all stars move on closed circular orbits parallel to the Galactic plane, and introduced two Oort constants, A and B, for describing the differential rotation of the Galaxy. In a galactocentric cylindrical coordinate system, these two parameters are given as

$$A = \frac{1}{2}\left(\frac{\partial V_\theta}{\partial R} - \frac{V_\theta}{R}\right)_{R=R_0}, \tag{1}$$

$$B = \frac{1}{2}\left(\frac{\partial V_\theta}{\partial R} + \frac{V_\theta}{R}\right)_{R=R_0}. \tag{2}$$

Here, R is measured from the Galactic center, R_0 is the galactocentric distance of the Sun. The azimuthal angle θ is reckoned counterclockwise. The combinations of the two constants give the rotational velocity of the LSR defined by the stars under consideration and its gradient at the Sun,

$$V_0 = -V_\theta = (A - B)R_0, \tag{3}$$

$$A + B = \left(\frac{\partial V_\theta}{\partial R}\right)_{R=R_0}. \tag{4}$$

The classical axisymmetric Oort method is easily generalized to an asymmetric model (Chandrasekhar 1942). In the two-dimensional case, we suppose that all stars move on orbits parallel to the Galactic plane. Then, the Oort constants can be expressed as

$$A = \frac{1}{2}\left(\frac{\partial V_\theta}{\partial R} - \frac{V_\theta}{R} + \frac{1}{R}\frac{\partial V_R}{\partial \theta}\right)_{R=R_0}, \tag{5}$$

$$B = \frac{1}{2}\left(\frac{\partial V_\theta}{\partial R} + \frac{V_\theta}{R} - \frac{1}{R}\frac{\partial V_R}{\partial \theta}\right)_{R=R_0}, \tag{6}$$

$$C = \frac{1}{2}\left(\frac{\partial V_R}{\partial R} - \frac{V_R}{R} - \frac{1}{R}\frac{\partial V_\theta}{\partial \theta}\right)_{R=R_0}, \tag{7}$$

$$K = \frac{1}{2}\left(\frac{\partial V_R}{\partial R} + \frac{V_R}{R} + \frac{1}{R}\frac{\partial V_\theta}{\partial \theta}\right)_{R=R_0}. \tag{8}$$

The parameters A and C denote the azimuthal and radial strain (shear) of the velocity field, respectively, B characterizes the vorticity (rotation), and K implies the local contraction (or expansion). This model is often applied to analyze the radial velocity data, while local expansion cannot be significantly determined just from the proper motion analysis.

In our previous work, we have given a three-dimensional asymmetric model by using the first-order expansion with 12 kinematical parameters to characterize the local Galactic velocity field (Zhu 2000). In this model, both proper motions and radial velocities of stars are needed to derive all 12 kinematical components, including three components for solar motion with respect to the LSR defined by stars considered. A detailed description has been given by Zhu (2000). The other nine kinematical parameters consisting of three components of vorticity ($D^-_{32}, D^-_{13}, D^-_{21}$), three components of strain velocity ($D^+_{32}, D^+_{13}, D^+_{12}$), and three additional components of Galactic expansion and/or contraction ($D^+_{11}, D^+_{22}, D^+_{33}$), are given by

$$D^+_{12} = \frac{1}{2}\left(\frac{\partial V_\theta}{\partial R} - \frac{V_\theta}{R} + \frac{1}{R}\frac{\partial V_R}{\partial \theta}\right)_{R=R_0}, \tag{9}$$

$$D^-_{21} = \frac{1}{2}\left(\frac{\partial V_\theta}{\partial R} + \frac{V_\theta}{R} - \frac{1}{R}\frac{\partial V_R}{\partial \theta}\right)_{R=R_0}, \tag{10}$$

$$D^+_{13} = -\frac{1}{2}\left(\frac{\partial V_R}{\partial z} + \frac{\partial V_z}{\partial R}\right)_{R=R_0}, \tag{11}$$

$$D^-_{13} = -\frac{1}{2}\left(\frac{\partial V_R}{\partial z} - \frac{\partial V_z}{\partial R}\right)_{R=R_0}, \tag{12}$$

$$D^+_{32} = -\frac{1}{2}\left(\frac{1}{R}\frac{\partial V_z}{\partial \theta} + \frac{\partial V_\theta}{\partial z}\right)_{R=R_0}, \tag{13}$$

$$D^-_{32} = -\frac{1}{2}\left(\frac{1}{R}\frac{\partial V_z}{\partial \theta} - \frac{\partial V_\theta}{\partial z}\right)_{R=R_0}, \tag{14}$$

$$D^+_{11} = \left(\frac{\partial V_R}{\partial R}\right)_{R=R_0}, \tag{15}$$

$$D^+_{22} = \left(\frac{V_R}{R} + \frac{1}{R}\frac{\partial V_\theta}{\partial \theta}\right)_{R=R_0}, \tag{16}$$

$$D^+_{33} = \left(\frac{\partial V_z}{\partial z}\right)_{R=R_0}. \tag{17}$$

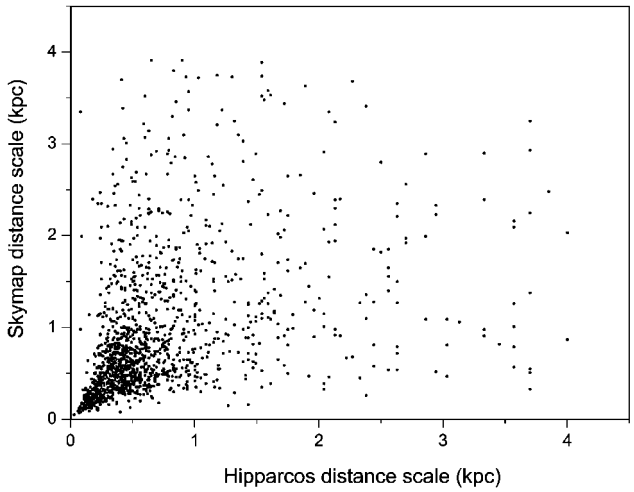

Fig. 1 Hipparcos and Skymap distance scales.

Note that the coefficients D_{12}^{+} and D_{21}^{-} are identical to the Oort constants A and B defined by Equations (5) and (6). The constants C and K are provided by the combinations of D_{11}^{+} and D_{22}^{+}:

$$C = \frac{1}{2}\left(D_{11}^{+} - D_{22}^{+}\right), \quad K = \frac{1}{2}\left(D_{11}^{+} + D_{22}^{+}\right), \tag{18}$$

or

$$D_{11}^{+} = K + C, \quad D_{22}^{+} = K - C. \tag{19}$$

For the thin disk population of stars, the derivative along z-axis is impossible to be meaningfully determined, thus, we have $\partial/\partial z = 0$. Suppose $V_z = 0$, the three-dimensional model of Equations (9)–(17) is easily generalized to a non-axisymmetric model of Equations (5)–(8). Similarly, we can simplify the asymmetric rotation model of Equations (5)–(8) to the circular rotation model of Equations (1) and (2).

In the following, the analysis is based on the 3-D model to re-examine the local velocity of the O-B stars at heliocentric distances of up to 3 kpc.

3 THE SAMPLE

The astrometric data were taken from the Hipparcos Catalogue, including proper motions and trigonometric parallaxes of stars. In order to obtain reliable spectral types, luminosity classes, and spectroscopic parallaxes, the Skymap Catalogue (Slater & Hashmall 1992), which contains 248 558 stars was used. The radial velocity data were taken from the General Catalog of mean radial velocities (Barbier-Brossat & Figon 2000) which contains 36 145 stars. Carrying out cross-identification, we found 2164 O-B stars common to three catalogues. Among them, 209 Hipparcos stars have no parallax measurements or negative parallaxes, and 365 stars belong to binaries, multiples, or suspected non-single systems indicated by the Hipparcos catalogue.

In order to inspect the systematic deviation of the distance scales which might disturb the velocity field for kinematical analysis, we compared the Hipparcos distance scale with the Skymap distance scale. Figure 1 shows the differences of the two systems. Statistically, the Hipparcos distance scale is smaller than that of the Skymap by about 10% on the average.

It is well known that the Gould-belt stars are embedded in the solar vicinity, which are O-A type stars younger than 3×10^7 years and exhibit quite different features in both their spatial distribution and kinematics (Westin 1985). The presence of a positive K-term was recognized as the main kinematical characteristic of the Gould Belt. This system has an inclination some 20° with respect to the Galactic

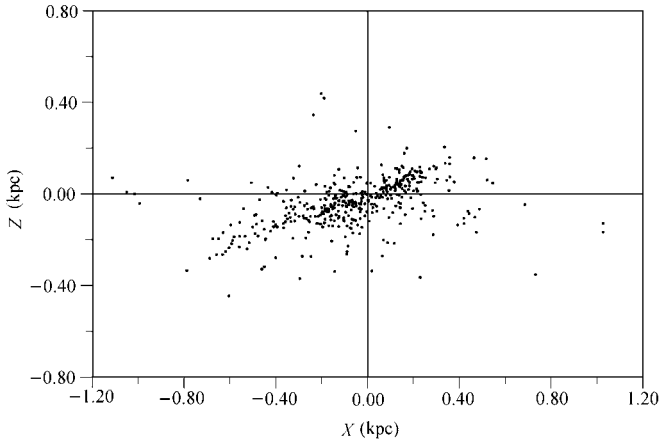

Fig. 2 Gould-belt stars projected on the XZ plane.

equator. Kinematical analyses of Gould-belt stars were recently performed by several authors (Torra et al. 2000; Comerón 1999), and are outside the scope of our present work. In order to avoid the disturbance from the Gould-belt stars, we picked out and removed 363 individual stars found in the present sample. Figure 2 displays the orientation and extent of the Gould-belt system, projected on the plane perpendicular to the Galactic plane. The X-axis is pointing to the Galactic center from the Sun and the Z-axis is positive in the direction to the north Galactic pole.

To ensure our sample belongs to the young disk population of stars, we selected O-B5 stars of all luminosity classes and B5-A0 stars of luminosity classes I-II in the following analysis, excluding the Gould-belt stars mentioned above.

4 ANALYSIS PROCEDURES

We apply the 3-D model discussed in Section 2 to derive the 12 kinematical parameters for the O-B stars. The equation of condition was given by Zhu (2000). These parameters are to be solved via the generalized least-squares method, for the known positions, proper motions, radial velocities and heliocentric distances. Prior to applying the least-squares to derive the unknowns, several points regarding the sampling domain of stars should be carefully considered.

It is well known that the velocity field of the Galaxy is characterized by an overall rotation, and, for a given group of stars, by their velocity dispersion and asymmetric drift velocity. Statistically, the velocity dispersion is proportional to the reciprocal of the heliocentric distance,

$$\sigma^2_{\kappa\mu^*_\ell} = \frac{1}{r^2}\left(\alpha^2\sin^2(\ell-\ell_v)+\beta^2\cos^2(\ell-\ell_v)\right), \tag{20}$$

$$\sigma^2_{\kappa\mu_b} = \frac{1}{r^2}\left(\alpha^2\cos^2(\ell-\ell_v)\sin^2 b+\beta^2\sin^2(\ell-\ell_v)\sin^2 b+\gamma^2\cos^2 b\right), \tag{21}$$

$$\sigma^2_{v_r/r} = \frac{1}{r^2}\left(\alpha^2\cos^2(\ell-\ell_v)\cos^2 b+\beta^2\sin^2(\ell-\ell_v)\cos^2 b+\gamma^2\sin^2 b\right), \tag{22}$$

where, the proper motion is in units of mas yr^{-1}, r is the heliocentric distance in kpc, κ=4.74047. The radial velocity is given in km s^{-1}, and α, β and γ are the semi-axes of the velocity ellipsoid. The longest axis deviates from the center-anticenter direction by the vertex deviation ℓ_v. Values of the semi-axes of the velocity ellipsoid and of the vertex deviation derived from the observations, were given by Binney & Merrifield (1998). It is easy to understand from Equations (20)–(22) that the random motion of stars at the solar vicinity dominates the systematic motion with respect to the LSR. To avoid such localized disturbances as well as disturbances from various known streams in the solar neighborhood, we set the lower limit of the heliocentric distance for the present sample at $r = 0.2$ kpc.

The youngest B6-A0 supergiants, bright giants and O-B5 stars belong to the thin disk population of stars of the Galaxy with a typical scale height of about 0.1–0.2 kpc. A meaningful determination of the velocity gradient along the direction perpendicular to the Galactic plane is impossible due to the small scale height. So we put $\partial V_R/\partial z = \partial V_\theta/\partial z = \partial V_z/\partial z = 0$. Inspecting the correlation coefficients among the 12 parameters, this point has been proved by a testing solution. Referring to Equations (11)–(14) and Equation (17), we have additional constraints for the present sample of stars

$$D_{13}^{+} = -D_{13}^{-} = -\frac{1}{2}\left(\frac{\partial V_z}{\partial R}\right)_{R=R_0}, \tag{23}$$

$$D_{32}^{+} = +D_{32}^{-} = -\frac{1}{2}\left(\frac{1}{R}\frac{\partial V_z}{\partial \theta}\right)_{R=R_0}, \tag{24}$$

$$D_{33}^{+} = 0. \tag{25}$$

Then, we have only nine parameters in total to be determined, comprising the three parameters of the solar motion (u_0, v_0, w_0) and the six parameters of the Galactic interior motion (D_{32}^{-}, D_{13}^{-}, D_{21}^{-}, D_{12}^{+}, D_{11}^{+}, D_{22}^{+}).

Measurement errors in the proper motion, parallax and radial velocity, introduce errors in the star's spatial velocity. In order to exclude stars with particularly large errors in the transverse and radial velocities or particularly large random motions, we introduce a numerical filter, $|\varepsilon|$. Considering both the measurement errors and the random velocities given by Binney & Merrifield (1998), we set $|\varepsilon|$ = 50 km s^{-1}. In our analysis, the filter automatically excludes those stars whose residual spatial velocities are larger than $|\varepsilon|$.

Due to the complexities arising from the measurement errors and stellar velocity dispersions, it is difficult to establish a reasonable mathematical weighting model. In the present analysis, we use the simple fitting errors from our model to calculate the weights. Initially, we adopt a constant weight. Having determined the initial values of the kinematical parameters, we calculate the residuals of the three velocity components. In an iterative fashion, this yields the weights for our analysis. The final solution gives estimated values of the kinematical parameters as well as their standard errors.

5 SOLUTIONS

The kinematical parameters are to be solved on the basis of the discussions in Sections 2–4. In order to inspect what difference the adopted distance scale makes, two experiments were made. In the first, we took the distance scale from Skymap spectroscopic measurements and the solutions are given in Table 1. In the second, we replaced the spectroscopic distance scale by that obtained from the Hipparcos trigonometric parallax measurements, and the solutions are given in Table 2. The first row of the each solution gives the total number of stars considered and the number of stars in each final solution after applying the numerical filter $|\varepsilon|$. In each of the two tables, the solutions refer to different subsets of our sample. First, the radial velocities complemented with Hipparcos proper motions for all O-B5 stars, B6-A0 supergiants and bright giants (luminosity classes I and II) for distances $r \geq 0.2$ kpc, and excluding the Gould-belt stars define the subset S1. It is noticeable that the stars of S1 are distributed mainly within 3 kpc of the Sun, with only a few out to $\sim$5 kpc.

Now, the first-order expansion of the velocity field given by our model may not be valid at a large heliocentric distance. Also, the error of the distance estimate may be increased at the large distance, especially for the distance estimates from the Hipparcos trigonometric parallax. To avoid these disturbances, we set the upper limit of the heliocentric distance at $r = 3.0$ kpc. The subset S1 restricted to the distance range 0.2 kpc $\leq r \leq$ 3.0 kpc, defines our subset S2. Next, considering the short time base of observation by the Hipparcos satellite (37 months), the proper motions for binaries might not be reliable. To avoid any disturbance from such stars, we exclude all such data and obtain the subset S3 (heliocentric distances 0.2 kpc $\leq r \leq$ 3.0 kpc).

Our subset S4 consists of all O-B5 stars (and no later types) in the heliocentric distance range 0.2–3.0 kpc, including the binaries. Finally, our subset S5 is S4 after excluding the binaries. All the solutions derived from the different subsets of stars are collected in Tables 1 and 2.

Within each of the two tables (Table 1 or Table 2), all the solutions for the five different subsets are in good mutual agreement for all the nine parameters. Recall that Solutions S1, S2 and S3 refer to a mixed sample of O-B5 stars and B6-A0 supergiants and bright giants, while solution S4 and S5 are obtained from the pure O-B5 stars. The kinematical solutions show that O-B5 stars, B6-A0 supergiants and bright giants are characterized by the same kinematics. Comparing solutions S1, S2 and S4 with solutions S3 and

Table 1 Kinematical solutions from proper motions and radial velocities of O-B stars based on the Skymap spectroscopic distance scale.

	S1	S2	S3	S4	S5
No. of stars	1611 (1499)	1522 (1450)	1254 (1192)	1406 (1345)	1150 (1099)
u_0 (km s^{-1})	11.51±0.39	11.52±0.40	11.53±0.47	11.51±0.41	11.57±0.50
v_0 (km s^{-1})	14.45±0.38	14.44±0.40	14.08±0.48	14.24±0.41	13.84±0.49
w_0 (km s^{-1})	7.81±0.39	7.81±0.41	7.86±0.47	7.74±0.41	7.79±0.50
D_{32}^{-} (km s^{-1} kpc^{-1})	1.27±0.50	1.31±0.52	1.21±0.60	1.24±0.54	1.08±0.63
D_{13}^{-} (km s^{-1} kpc^{-1})	0.03±0.58	0.04±0.59	–0.13±0.68	0.07±0.62	–0.09±0.73
D_{21}^{-} (km s^{-1} kpc^{-1})	–16.16±0.77	–16.19±0.78	–15.92±0.91	–16.21±0.82	–15.94±0.97
D_{12}^{+} (km s^{-1} kpc^{-1})	12.76±0.76	12.86±0.79	13.08±0.91	13.08±0.83	13.31±0.96
D_{11}^{+} (km s^{-1} kpc^{-1})	–2.34±1.15	–2.51±1.18	–3.10±1.37	–2.78±1.25	–3.53±1.46
D_{22}^{+} (km s^{-1} kpc^{-1})	–1.79±1.00	–1.87±1.04	–2.53±1.20	–2.14±1.08	–2.90±1.26

Table 2 Kinematical solutions from proper motions and radial velocities of O-B stars based on the Hipparcos distance scale.

	S1	S2	S3	S4	S5
No. of stars	1381 (1293)	1328 (1281)	1103 (1063)	1214 (1171)	1001 (964)
u_0 (km s^{-1})	10.64±0.36	10.64±0.36	10.41±0.41	10.68±0.38	10.62±0.45
v_0 (km s^{-1})	11.49±0.35	11.48±0.37	11.65±0.42	11.45±0.39	11.63±0.45
w_0 (km s^{-1})	6.38±0.35	6.38±0.36	6.46±0.42	6.32±0.38	6.35±0.46
D_{32}^{-} (km s^{-1} kpc^{-1})	1.31±0.56	1.31±0.56	1.19±0.64	1.34±0.59	1.20±0.68
D_{13}^{-} (km s^{-1} kpc^{-1})	–0.52±0.66	–0.53±0.66	–0.65±0.75	–0.45±0.71	–0.62±0.81
D_{21}^{-} (km s^{-1} kpc^{-1})	–14.73±0.85	–14.74±0.87	–14.67±0.98	–14.81±0.92	–14.76±1.06
D_{12}^{+} (km s^{-1} kpc^{-1})	16.30±0.86	16.32±0.86	16.37±0.98	16.19±0.93	16.18±1.06
D_{11}^{+} (km s^{-1} kpc^{-1})	–4.11±1.31	–4.11±1.32	–3.92±1.50	–3.82±1.42	–4.00±1.63
D_{22}^{+} (km s^{-1} kpc^{-1})	–4.21±1.11	–4.26±1.12	–4.24±1.27	–4.14±1.18	–4.03±1.36

S5, where the first three are for stars including binary and multiple systems, and the last two are for stars with all suspected non-single systems excluded, we find that the Hipparcos proper motions for binaries do not disturb our kinematical solution drastically, as we suspected before (cf. Miyamoto & Zhu 1998), even though the proper motions were derived from observations in a short-time span of less than 37 months.

Recall again that the solutions in Tables 1 and 2 are derived from stars on different distance scales, namely the spectroscopic and the Hipparcos distance scales. Comparing the solutions in Tables 1 and 2, we find the kinematical parameters strongly depended on the distance scale adopted. It is revealed that the Hipparcos distance scale is about 10% lower than the spectroscopic distance scale. In our previous work (Miyamoto & Zhu 1998), we have discussed the effect of the distance estimate in the proper motion analysis. In that case the distance estimate directly influences the determination of the solar motion, but only indirectly influences the determination of the parameters $D_{ij}^{\pm}$ through the solar motion. In analyzing the radial velocities, however, the case is just the opposite. Such a feature is easily inferred from the matrix elements given by equations (17)–(21) by Zhu (2000), and has been confirmed by inspecting the correlation coefficients among the parameters to be determined. For this complex effect, we have the following conclusions: (a) a lower distance scale results in decreasing the absolute values of the parameters of the solar motion (u_0, v_0, w_0), and increasing the absolute values of (D_{12}^{+}, D_{11}^{+}, D_{22}^{+}); (b) due to the small scale height of the young disk population of O-B stars, all the stars considered here are located close to the Galactic plane at very low Galactic latitude b. Thus, the parameters $D_{32}^{-}(= D_{32}^{+})$ and $D_{13}^{-}(= -D_{13}^{+})$ are only weakly correlated with the distance scale; (c) similar to the asymmetric drift, the lower the solar motion component v_0 is, the faster the Galactic rotational speed will be, and the rotational velocity of the Galaxy is proportional to $(D_{12}^{+} - D_{21}^{-})$. Therefore, the lower distance scale gives a lower estimate of the solar motion component v_0, which indirectly leads to an increase of the value $(D_{12}^{+} - D_{21}^{-})$.

Another serious problem is the low precision of the distance measurements. Inspecting the Hipparcos trigonometric parallaxes, we find that a majority of stars in the present wide distance range domain have relative errors σ_π/π of Hipparcos parallaxes larger than 1. The Skymap spectroscopic distances were taken from different sources, which makes it hard to evaluate their uncertainty. When we plot the two different distance scales one against the other, a tremendous scatter is shown (Figure 1), and the scatter is more

pronounced for the distant stars. Instead of the spectroscopic distance scale, Miyamoto et al. (1993) tried to use a distance scale calibrated by photometric measurement of the O-B5 stars. They found the distance scale estimated from the photometric calibration is smaller than that of Skymap by about 5%. Thus, their distance scale is systematically closer to that of Hipparcos.

Note that the parameter D_{13}^- is practically zero for all the solutions. Thus, we will confine ourselves to deal with the other eight parameters in the following discussion.

6 CONCLUDING DISCUSSION

Because the different subset of stars (when on the same distance scale) give such highly consistent solutions of the kinematical parameters, we can just take any one of the five solutions for the following discussion. We prefer to take the large size S2 of O-B5 stars, B6-A0 supergiants and bright giants in distance range $0.2\,\mathrm{kpc} \leq r \leq 3.0\,\mathrm{kpc}$.

The total velocity of the Sun S_0 relative to the LSR defined by the stars considered, with the apex towards ℓ_0 and b_0, derived on the basis of the Skymap distance scale, is

$$S_0 = 20.1 \pm 0.4\ \mathrm{km\,s^{-1}}, \quad \ell_0 = 51.2^\circ \pm 1.2^\circ, \quad b_0 = +22.9^\circ \pm 1.1^\circ, \tag{26}$$

while based on the Hipparcos distance scale, is

$$S_0 = 16.9 \pm 0.4\ \mathrm{km\,s^{-1}}, \quad \ell_0 = 47.2^\circ \pm 1.3^\circ, \quad b_0 = +22.2^\circ \pm 1.2^\circ. \tag{27}$$

Our previous determination of the solar motion gave

$$S_0 = 19.1 \pm 0.5\ \mathrm{km\,s^{-1}}, \quad \ell_0 = 49.2^\circ \pm 1.6^\circ, \quad b_0 = +21.9^\circ \pm 1.3^\circ, \tag{28}$$

which was obtained from a proper motion analysis of O-B5 stars based on the Skymap distance scale (Miyamoto & Zhu 1998). The present determinations coincide with the previous one within the standard errors, except the total solar motion based on the Hipparcos distance scale.

The parameters D_{12}^+ and D_{21}^- are identical to the Oort constants A and B in the circular model. Then we have

$$\omega_0 = A - B = -\left(\frac{V_\theta}{R}\right)_{R=R_0} = 29.05 \pm 1.11\ \ \mathrm{km\,s^{-1}\,kpc^{-1}}, \tag{29}$$

$$A + B = \left(\frac{\partial V_\theta}{\partial R}\right)_{R=R_0} = -3.34 \pm 1.11\ \ \mathrm{km\,s^{-1}\,kpc^{-1}} \tag{30}$$

for the Skymap distance scale; and

$$\omega_0 = A - B = -\left(\frac{V_\theta}{R}\right)_{R=R_0} = 31.05 \pm 1.22\ \ \mathrm{km\,s^{-1}\,kpc^{-1}}, \tag{31}$$

$$A + B = \left(\frac{\partial V_\theta}{\partial R}\right)_{R=R_0} = 1.58 \pm 1.22\ \ \mathrm{km\,s^{-1}\,kpc^{-1}} \tag{32}$$

for the Hipparcos distance scale. Here $(A + B)$ expresses the slope of the rotation curve at the Sun. It indicates that the variation of the distance scale does not only change the rotational speed of the Galaxy, but also changes its gradient at the Sun.

Carrying out a proper-motion analysis for Hipparcos O-B5 stars, we found a clear warping motion that is a systematic rotation $+3.8 \pm 1.1$ km s^{-1} kpc^{-1} of stars about the axis pointing to the Galactic center (Miyamoto & Zhu 1998). The present analysis gives

$$2D_{32}^- = -\left(\frac{1}{R}\frac{\partial V_z}{\partial \theta}\right)_{R=R_0} = +2.6 \pm 1.0\ \ \mathrm{km\,s^{-1}\,kpc^{-1}} \tag{33}$$

on the Skymap distance scale, and

$$2D_{32}^- = -\left(\frac{1}{R}\frac{\partial V_z}{\partial \theta}\right)_{R=R_0} = +2.6 \pm 1.1\ \ \mathrm{km\,s^{-1}\,kpc^{-1}} \tag{34}$$

on the Hipparcos distance scale. The determination of the warping motion is fortunately independent of the distance scale adopted, as we discussed before.

The K-term is derived from a combination of the parameters D^+_{11} and D^+_{22}. On the Skymap distance scale, we have

$$K = \frac{1}{2}\left(D^+_{11} + D^+_{22}\right) = -2.2 \pm 0.8 \ \mathrm{km\,s^{-1}\,kpc^{-1}}; \tag{35}$$

while on the Hipparcos distance scale, we have

$$K = \frac{1}{2}\left(D^+_{11} + D^+_{22}\right) = -4.2 \pm 0.9 \ \mathrm{km\,s^{-1}\,kpc^{-1}}. \tag{36}$$

A negative K-term means an overall contraction of stars in the solar vicinity. The existence of a mean positive K-term associated with the earliest type Gould-belt stars in the solar neighborhood has long been recognized. This trend in the motion of the earliest type stars has been taken as evidence for expansion of the local system at the solar vicinity. Comerón et al. (1994) have examined the local kinematical structure of the O-B stars, and found that stars with within 1.5 kpc of the sun exhibit a contraction, while stars within 0.4 kpc show an expansion that may be dominated by the moving groups. A recent work by Bobylev (2004) confirmed that a negative K-term exists in the distant O-B stars. It should be noted that our present work differs from both Comerón et al. and Bobylev, because we have already removed Gould-belt stars from our sample.

In general, we conclude that the kinematical structure of O-B stars other than the Gould-belt stars, exhibits an overall rotation around the Galactic gravitation center on the Galactic plane simultaneously with a warping motion and a contraction. The adopted distance scale plays an important role in characterizing the kinematical parameters at the present level of the measurement uncertainty.

Acknowledgements This work was supported by the National Natural Science Foundation of China (Grant 10333050) and by Nanjing University Talent Development Foundation.

References

Backer D. C., Sramek R. A., 1999, ApJ, 524, 805
Barbier-Brossat M., Figon P., 2000, A&AS, 142, 217
Binney J., Merrifield M., 1998, Galactic Astronomy, Princeton: Princeton University Press, p.633
Bobylev V. V., 2004, Astronomy Letters, 30, 159
Caldwell J. A. R., Coulson I. M., 1987, AJ, 93, 1090
Chandrasekhar, S., 1942, Principles of Stellar Dynamics, Princeton: Princeton Univ. Press
Comerón F., 1999, A&A, 351, 506
Comerón F., Torra J., Gómez A. E., 1994, A&A, 286, 789
Drimmel R., Smart R. L., Lattanzi M. G., 2000, A&A, 354, 67
Feast M., Catchpole R. M., 1997, MNRAS, 286, L1
Feast M., Whitelock P., 1997, MNRAS, 291, 683
Kerr F. J., 1957, AJ, 62, 93
Kerr F. J., Linden-Bell D., 1986, MNRAS, 221, 1023
Méndez R. A., Platais I., Girard T. M. et al., 1999, ApJ, 524, L39
Metzger M. R., Caldwell J. A. R., Schechter P. L., 1998, AJ, 115, 635
Miyamoto M., Sôma M., Yoshizawa M., 1993, AJ, 105, 2138
Miyamoto M., Zhu Z., 1998, AJ, 115, 1483
Olling R. P., Dehnen W., 2003, ApJ, 599, 275
Pont F., Mayor M., Burki G., 1994, A&A, 285, 415
Pont F., Queloz D., Bratschi P., et al., 1997, A&A, 318, 416
Slater M., Hashmall J., 1992, Skymap Star Catalog, version 3.7 (Doc. 544-FDD-89/001R3UD1), Goddard Space Flight Center, Greenbelt, MD
Smart R. L., Drimmel R., Lattanzi M. G., et al., 1998, Nature, 392, 471
Torra J., Fernández D., Figueras F., 2000, A&A, 359, 82
Westin T. N. G., 1985, A&AS, 60, 99
Zhu Z., 2000, Ap&SS, 271, 353